IEEE Access
Multidisciplinary | Rapid Review | Open Access Journal

Received June 29, 2018, accepted July 12, 2018, date of publication July 17, 2018, date of current version August 15, 2018.

Digital Object Identifier 10.1109/ACCESS.2018.2856742

Accuracy and Precision of Edge-Based Modulation Transfer Function Measurement for Sampled Imaging Systems

KENICHIRO MASAOKA
Japan Broadcasting Corporation (NHK), Tokyo 157-8510, Japan
e-mail: masaoka.k-gm@nhk.or.jp

ABSTRACT The real-time, edge-based, multidirectional modulation transfer function (MTF) measurement system has elucidated the MTF characteristics of sampled imaging systems. However, the accuracy and precision of edge-based MTF measurements are not well understood quantitatively because of the complicated shift-variant nature of the sampling process by the image sensor and the binning process in the edge-based method for producing a supersampled edge spread function. The edge-based MTF measurement is valid only when the edge positions imaged are assumed to be distributed uniformly relative to the sampling sites. This study demonstrates that precision, which is dependent on the edge angle, is counterintuitively high at a higher oversampling ratio of the binning regardless of the smaller pixel counts per bin even with camera noise, and that significantly high precision can be achieved by taking an ensemble average of MTFs computed over a single cycle of the binning phase, even at low oversampling ratios, with high accuracy through proper corrections to compensate for the attenuation of the MTF values due to the discrete processing of the edge-based method.

INDEX TERMS Modulation transfer function, superresolution.

I. INTRODUCTION

Great efforts are being exerted toward the development of ultra-high-definition (UHD) infrastructure and to deliver broadcast 4K/8K content to homes. In addition to broadcasting, 8K technology is imperative for virtual reality development in addition to education, security, and medical applications. UHD relies on the spatial resolution characteristics beyond those of HD to offer lifelike visual perception or ''realness'' [1], thereby addressing the challenges in 4K/8K camera performance.

Spatial resolution is the ability of an imaging system to distinguish fine details; it is not the same as addressability or pixel resolution because no imaging system is perfect. The modulation transfer function (MTF) is a reliable indicator of the spatial performance of an optical system [2]. By analogy with optics, the spatial resolution of a sampled imaging system is generally characterized by an MTF [3]. The MTF of the overall system can be described elegantly as the product of all individual MTFs of its components when the given imaging system is approximately linear and shift invariant [4]. To maintain the convenience of the transfer function approach, it is assumed that the object being imaged has spatial frequency components with random phases that are distributed uniformly relative to the sampling sites [5], [6].

It has recently become possible to measure the MTF of a video camera in real time on the basis of its edge responses with arbitrary direction in a region of interest (ROI) [7]. Fig. 1 shows a schematic diagram of the MTF measurement system. The system comprises a stand-alone application and PC with frame memory fed with a serial digital interface (SDI) video signal within its linear range. This system enables accurate focusing and fine adjustment of flange focal distance in an objective manner by using solely the real-time MTF measurement results. The analysis of multidirectional edges on a starburst chart yields a contour plot of multidirectional MTFs that enables the direct observation of the anisotropy due to the performance and conditions of the camera and lens (e.g., misalignment of the optical axis of the lenses and image sensor), as well as the pixel arrangement of the image sensor and image processing (e.g., Bayer color filter array demosaicing). The contour plot in Fig. 1, whose radial coordinate represents the spatial frequency from zero to the Nyquist frequency, and the polar angle represents the edge

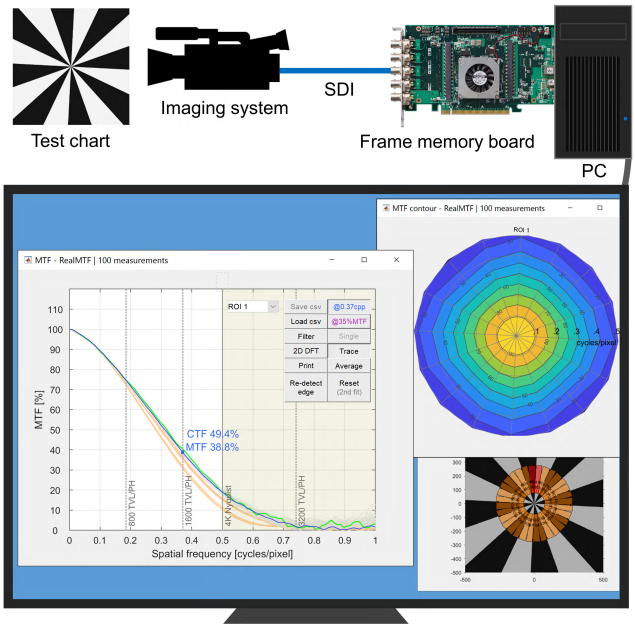

FIGURE 1. Schematic diagram of real-time MTF measurement system.

direction of the target, appears square-shaped at low MTF levels because the green pixels in the Bayer color filter array of the single-chip image sensor are sparse in the diagonal directions. Thus, the real-time MTF measurement system has further improved the knowledge of such MTF characteristics.

The present study focuses on the accuracy and precision of edge-based MTF measurement, which is complicated because of the shift-variant nature of the sampled imaging system itself and the binning process employed to yield a supersampled edge gradient. This paper provides simulation results on the accuracy and precision of edge-based methods over the whole edge angle range with various binning phases and oversampling ratios.

II. EDGE-BASED MTF MEASUREMENT METHODS

A. STANDARD EDGE-BASED METHOD

The ISO 12233 [8] edge-based method is intended to characterize the spatial resolution of digital still cameras with two-dimensional photoelement arrays that respond to light in proportion to the intensity of the light [9], [10]. The spatial frequency response is measured to approximate the MTF as a function of the horizontal or vertical spatial frequencies by analyzing an edge gradient of a single portion of an image of a knife-edge target whose edge is slanted relative to the pixel array. Note that the slanted edges in the ISO 12233 chart have 5° angles, and the ROI must be a rectangle with a slanted edge passing through the short sides. The edge angle in a vertical ROI is estimated by performing a simple linear regression on the collected row-to-row edge locations estimated by taking a one-dimensional derivative of the edge gradient in each row and finding the centroid at subpixel accuracy. The ROI pixels are then projected along the direction of the estimated edge onto the horizontal axis, which is divided into quarter-pixel-wide bins to reduce the influence of signal aliasing on the estimated MTF. Note that the bin array is not perpendicular to the edge direction. The values of the pixels collected in each bin are averaged to generate a $4\times$ oversampled one-dimensional edge spread function (ESF). A finite difference filter $[0.5\ 0\ -0.5]$ is used to approximate the one-dimensional derivative of the ESF to obtain a line spread function (LSF) After applying a Hamming window to the LSF, a discrete Fourier transform is performed. The modulus of the corresponding optical transfer function (OTF) is then normalized to unity at zero frequency, and the MTF is estimated over a range of horizontal or vertical spatial frequencies beyond the Nyquist frequency.

The MTF can be calculated in a wide range of spatial frequencies from a relatively small region via edge-based methods. However, it is more difficult to adjust the focus on a knife-edge target than on a bar chart accurately by visual observation. According to ISO 12233, camera focus should be set by performing a series of image captures at various focus settings and then selecting the setting that provides the highest average modulation level, which is time-consuming and error-prone. Furthermore, the edge angle estimation process is not robust against camera noise because the derivative of the data in each row in the ROI is taken to compute the position of the edge [11], which propagates as a bias error in the resultant MTF measurement [12]. The slant angle must also be small because a larger angle introduces more negative bias into the computed MTF [13].

B. NEW EDGE-BASED METHOD

The new edge-based method incorporated into the real-time MTF measurement system accepts any edge directions (not just near-horizontal and vertical) in arbitrarily shaped ROIs (not just rectangular); therefore, it accommodates tangential and sagittal measurements. Fig. 2 shows a schematic flow diagram of the new edge-based method. The algorithm uses the Sobel approximation to generate a binary edge image in an ROI. The edge angle is estimated roughly by performing a Hough transform at an angular resolution of 0.1°, and the ROI image is rotated by the estimated angle such that the edge is oriented approximately upright. This ROI rotation simply stabilizes the next fine edge angle prediction. The angle of the nearly vertical edge is estimated by fitting a parameterized two-dimensional normal cumulative distribution function to the ROI pixels with significantly higher accuracy, precision, and robustness against camera noise, without interpolating the ROI pixel values [11]. Thereafter, the ROI image is slightly rotated again, and the ROI pixels are dropped vertically into subpixel-wide bins aligned along the horizontal axis. Subsequently, a supersampled ESF is generated by averaging the pixel values in each bin. Each zero-count bin is interpolated by averaging the pixel values in the left nearest non-empty bin and the right neighbor bin. If both neighbors of a zero-count bin are non-empty bins, the value of the zero-count bin is padded by the mean value of the pixel values

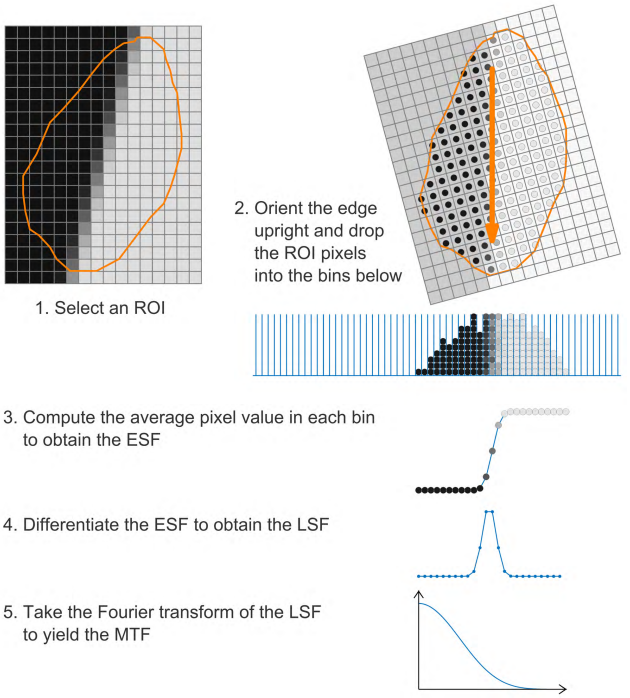

FIGURE 2. Schematic flow diagram of the new edge-based method. Wide bins and a small ROI are used as simple examples.

in the two neighbor bins, which provides a smooth ESF. For two or more consecutive zero-count bins, the bin(s) except for the rightmost bin is (are) padded with the mean values of the pixels in the left nearest non-empty bin, whereas the rightmost zero-count bin is padded with the mean value of the pixels in the left nearest non-empty bin and the right neighbor bin. A finite difference filter [0.5 0 −0.5] is used to approximate the one-dimensional derivative of the ESF to obtain an LSF. Thereafter, a Tukey window is applied to the LSF for apodization to better eliminate leakage error than by applying the Hamming window used in the ISO 12233 edge-based method. Normalizing the modulus of the OTF obtained from the LSF produces the MTF.

Other methods allow for MTF measurements at edge angles other than those along the vertical and horizontal directions. In the method proposed by Ojanen and Tervonen [14], a rotated rectangular ROI is roughly oriented to the edge angle and a derivative of the interpolated pixel values in each line parallel to the short side of the rectangular ROI is taken to detect the edge locations; however, this method is not robust against camera noise because of the derivative process. In the method proposed by Kohm [15], a Sobel edge-detection operator followed by thresholding and binary morphological processing and a least squares regression analysis of the detected edge locations is then performed to find the edge angle. However, this method is also not robust against camera noise because of the sampling of the edge locations.

The new real-time MTF measurement system averages the first input frames to reduce camera noise and improve the precision of the edge prediction. The bin locations corresponding to the ROI pixel positions computed in the projection process are recorded once in a lookup table (LUT) and then the ROI pixels are mapped to the bins based on the LUT in the subsequent input video frames without predicting the edge for each frame with camera noise under an assumption of that the edge angle is constant during the measurement. This significantly reduces the computational cost, enabling the system to compute MTFs at a speed of 60 frames per second when analyzing a single 100 (W) × 200 (H)-pixel rectangular ROI (this size is recommended by the Association of Radio Industries and Businesses [16]).

III. MEASUREMENT ACCURACY AND PRECISION OF EDGE-BASED METHODS

A. MTF FOR SAMPLED IMAGING SYSTEMS

For a sampled imaging system where sampling occurs on an equally spaced rectangular grid, Park *et al.* [5] argued that a rectangle function with widths that are equal to the sampling intervals in the horizontal and vertical directions should be convolved to the point spread function of the presampling imaging subsystem comprising the image-forming optics and sampling aperture. Boreman [6] followed this idea and defined a sinc-function "sampling MTF" as "a corresponding MTF component that are inherent in the sampling process itself by assuming that the scene being imaged is randomly positioned with respect to the sampling sites." However, the schematic diagrams in Fig. 4 of [5] and Fig. 2.12 of [6] are more about the MTF of an ideal rectangular sensor with a 100% fill factor, which is identical to a 2D sinc function of the sampling MTF. The MTF of a sampling aperture (or "aperture MTF" defined in ISO 15529 [4]) that performs the spatial averaging of scene irradiance that falls on it is referred to as a "detector-footprint MTF" in [6] aside from the sampling MTF. This sampling MTF does not generally contribute to the MTF measurements of sampled imaging systems.

When the spatial frequency ξ is given in cycles per pixel, the MTF $|F_s(\xi)|$ derived in an edge-based method is expressed as follows:

$$\begin{aligned}|F_s(\xi)| &= |\mathscr{F}\{\mathrm{step}(x-x_0) * f(x) * \mathrm{rect}(n_{\mathrm{bin}}x)\ \mathrm{comb}(n_{\mathrm{bin}}x) \\ &\quad * 0.5[\delta(x+1/n_{\mathrm{bin}}) - \delta(x-1/n_{\mathrm{bin}})]\}| \\ &= |e^{-j2\pi x_0\xi}(\delta(\xi)/2 + 1/j2\pi\xi)\ F(\xi)\ \mathrm{sinc}(\xi/n_{\mathrm{bin}}) \\ &\quad * \mathrm{comb}(\xi/n_{\mathrm{bin}})\ j\mathrm{sin}(2\pi\xi/n_{\mathrm{bin}})| \\ &= |\mathrm{sinc}(\xi/n_{\mathrm{bin}})\mathrm{sinc}(2\xi/n_{\mathrm{bin}})| \\ &\quad |e^{-j2\pi x_0\xi}F(\xi) * \mathrm{comb}(\xi/n_{\mathrm{bin}})|, \end{aligned} \tag{1}$$

where n_{bin} is the number of bins per original pixel width, i.e., the oversampling ratio, $F(\xi)$ is the Fourier transform $\mathscr{F}\{\ \}$ of LSF $f(x)$, and x_0 represents the binning phase relative to the pixel coordinates, which is not generally specified in edge-based methods. Forming a supersampled ESF introduces negative biases of $\mathrm{sinc}(\xi/n_{\mathrm{bin}})$ and $\mathrm{sinc}(2\xi/n_{\mathrm{bin}})$ due to the binning and derivative processes, respectively,

in the computed MTF [11], [17]. These negative biases are compensated by multiplying the inverse of the sinc functions with $|F_s(\xi)|$. Note that the sampling MTF is coincident with the negative bias of $\mathrm{sinc}(\xi/n_{\mathrm{bin}})$ by the binning in the edge-based method when $n_{\mathrm{bin}} = 1$ (i.e., no oversampling).

B. MTF CRITERIA AND ANALYSIS METHODOLOGY

Typically, the spatial resolution characteristics of a broadcast HD camera are measured by analyzing its square-wave pattern responses at specific horizontal spatial frequencies, where a bar-type resolution target is imaged to determine if the modulation meets a minimum threshold criterion, which is typically a contrast transfer function (CTF) of 45% at 800 TV lines per picture height (TVL/PH: twice the number of black and white line pairs or cycles across a distance equal to the picture height). The sine-wave-derived MTF value is approximated to roughly 35% by multiplying $\pi/4$ by the square-wave-derived CTF value based on Coltman's formula [18]. By being conservative and assuming that 4K/8K camera images are sometimes cropped to HD-sized images, it would be reasonable to adopt an MTF criterion of 35% by using the normalized spatial frequency of 0.37 cycles per pixel, which corresponds to 800 TVL/PH for HD, 1600 TVL/PH for 4K, and 3200 TVL/PH for 8K. This single-valued criterion is very useful for professional cameras because they usually have bell-shaped MTF curves. Note that $|\mathrm{sinc}(\xi)|^4$ is a useful function to approximate a typical MTF curve of high-performance 4K/8K cameras that satisfy the MTF criterion of 35% at 0.37 cycles/pixel [7]. The sinc function is also simple in the formula because it has a null point at the sampling frequency. Furthermore, it is easy to synthesize a knife-edge image with a $|\mathrm{sinc}(\xi)|^4$ MTF characteristic by applying a size-limited square averaging filter using a super resolution technique. In the following sections, a $|\mathrm{sinc}(\xi)|^4$ MTF characteristic is used for the accuracy and precision analysis of the edge-based methods.

C. ACCURACY OF THE ISO 12233 EDGE-BASED METHOD

In the edge-based methods, MTF compensation is required because of the negative biases due to the binning and derivative processes. However, correction for the binning has not yet been adopted in the ISO 12233 edge-based method, and the correction for the derivative was not mentioned in the original ISO 12233 published in 2000, whereas two different but incorrect sine-based equations were adopted in version 2 published in 2014 and version 3 published in 2017. Furthermore, larger slant angles lead to more negative biases [13]. Finally, the $|\mathrm{sinc}(\xi)|^4$ MTF value of 38.9% at 0.37 cycles/pixel is underestimated as 38.3% for the edge angle of 5° and 4× binning with the "correct" sinc-based correction for only the derivative. In addition to the negative biases, the shift-variant nature of the sampled imaging system and the binning process in the edge-based methods (including the new method) degrades precision, as discussed in the next section.

D. ACCURACY AND PRECISION OF THE NEW EDGE-BASED METHOD

The rationale for the 5° slant angle used in the ISO 12233 standard rather than another angle is provided in only very few studies [13], [19]. Regarding the binning, it has been argued that a 4× oversampling was the best choice to reduce noise and aliasing [12], [20], [21]. However, their analysis is limited in terms of the variation of binning phase and edge angle.

In the edge-based methods, an ESF is obtained by binning pixel values sampled at unequal intervals to represent a continuous response of $\mathrm{step}(x - x_0) * f(x)$ in (1). The precision of the MTF computed from the ESF depends on the binning phase and oversampling ratio. Fig. 3 shows the discrete and mean MTF curves estimated from a synthesized 100 (W) × 200 (H)-pixel image with a critical edge angle of $\tan^{-1}(1/4)$ (= 14.0362°) by using the new edge-based method with 4× and 8× binning ($n_{\mathrm{bin}} = 4$ and 8) at $(32n_{\mathrm{bin}})^{-1}$-interval binning phases, which correspond to x_0 in (1). The image was generated by convolving a 101 × 101-pixel averaging filter four times to a 101× supersampled binary image before downsampling to obtain an MTF characteristic of $|\mathrm{sinc}(\xi_x, \xi_y)|^4$. Here, the edge passed through the center of the image ($x_0 = 0$). In this simulation, the edge angle value was set manually (i.e., not predicted using the algorithm) to separate the edge prediction error factor from this analysis. In this case,

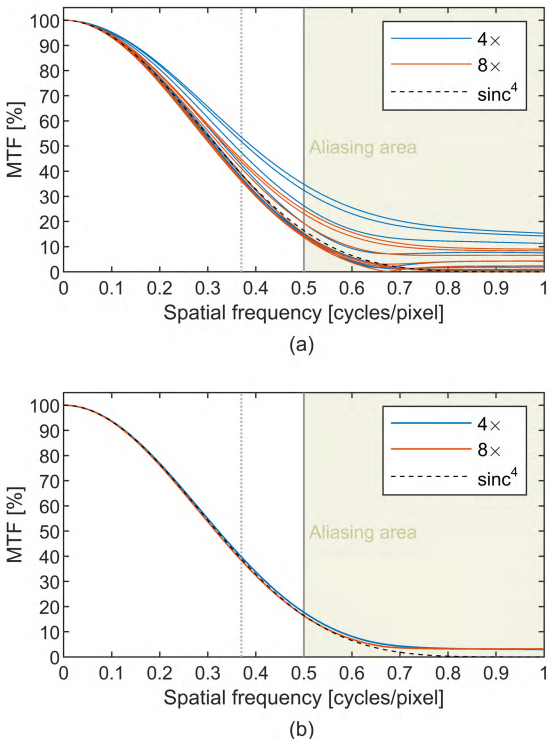

FIGURE 3. MTF curves estimated from synthesized 100 (W) × 200 (H)-pixel edge image with an edge angle of $\tan^{-1}(1/4)$ for 4× and 8× binning at $(32\ n_{\mathrm{bin}})^{-1}$-interval binning phases with the new edge-based method: (a) 32 discrete curves and (b) mean curve for each n_{bin}.

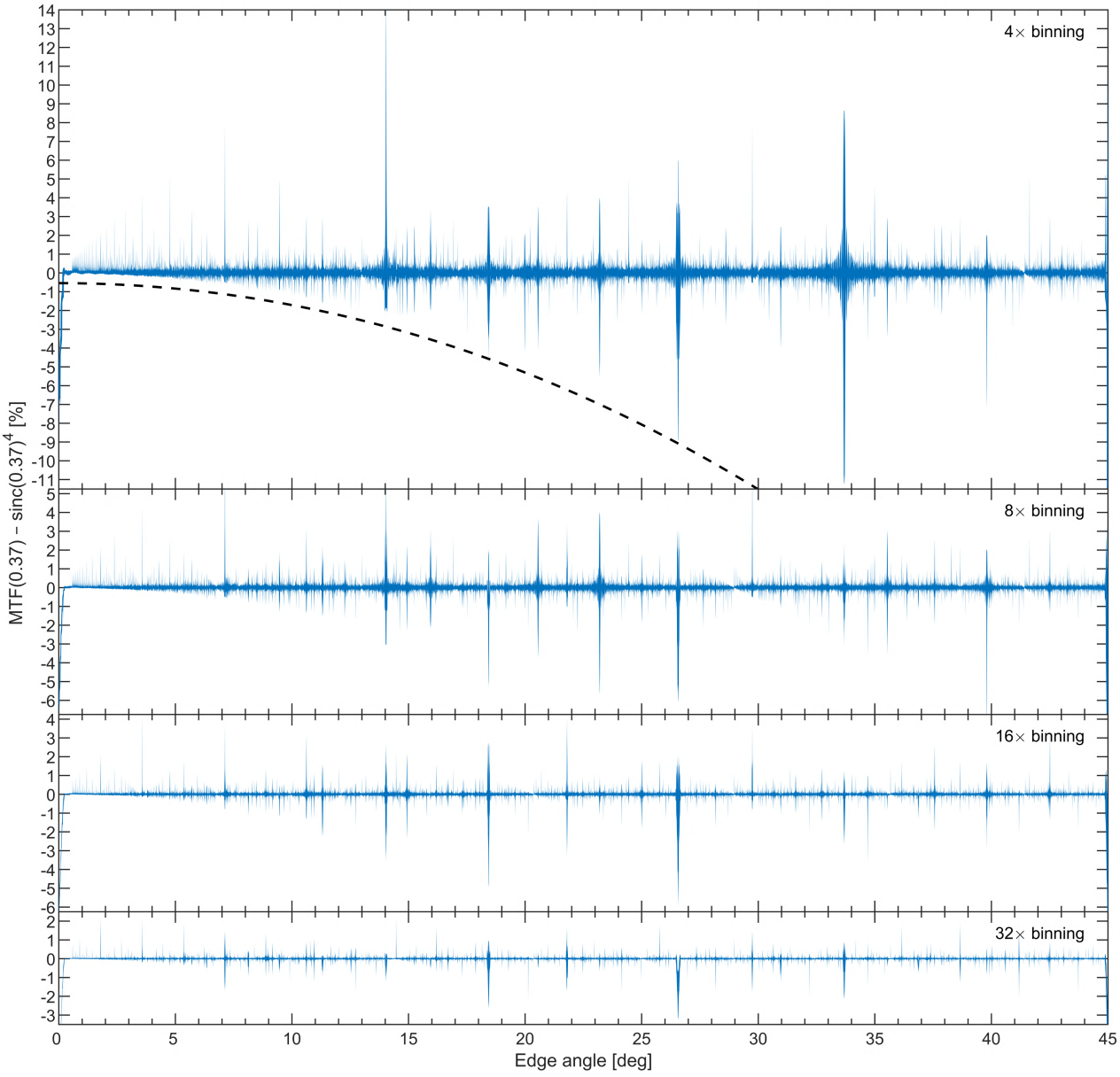

FIGURE 4. MTF error ranges at 0.37 cycles/pixel estimated from synthesized 200 (W) × 200 (H)-pixel edge image with the new edge-based method (blue) for 4×, 8×, 16×, and 32× binning at $(1024\ n_{\mathrm{bin}})^{-1}$-interval phases and with the ISO 12233 edge-based method (black dashed line) for 4× binning.

the MTF results for 4× binning are more diverse than those for 8× binning, whereas the mean MTF curves are close to $|\mathrm{sinc}(\xi_x, \xi_y)|^4$.

The precision of the edge-based methods also depends on the edge angle. Considering the mirror and rotational symmetry of the square grid sampling, edge angles ranging from 0° to 45° at 0.01° intervals and critical edge angles with edge slopes corresponding to simple fractions with two positive integers ranging from 1 to 100 were analyzed with different binning phases at $(1024n_{\mathrm{bin}})^{-1}$ intervals with the new edge-based method for n_{bin} values of 4, 8, 16, and 32. The edge angle values were set manually. Fig. 4 shows the estimated MTF error ranges at 0.37 cycles/pixel estimated from a synthesized 200 (W) × 200 (H)-pixel image for each n_{bin}. Fig. 4 also shows a combined MTF error of the negative biases caused by the binning and edge angle in the ISO 12233 edge-based method with an n_{bin} value of 4. Significantly high accuracy is observed for the new edge-based method. Regarding precision, it may be counterintuitive that the MTF estimates with large oversampling ratios are generally more precise regardless of the more frequent zero-count bin pixels with the simple interpolation. However, it is convincing if one considers that 4× binning is approximately the binning of every bin pair of 8× binning, and

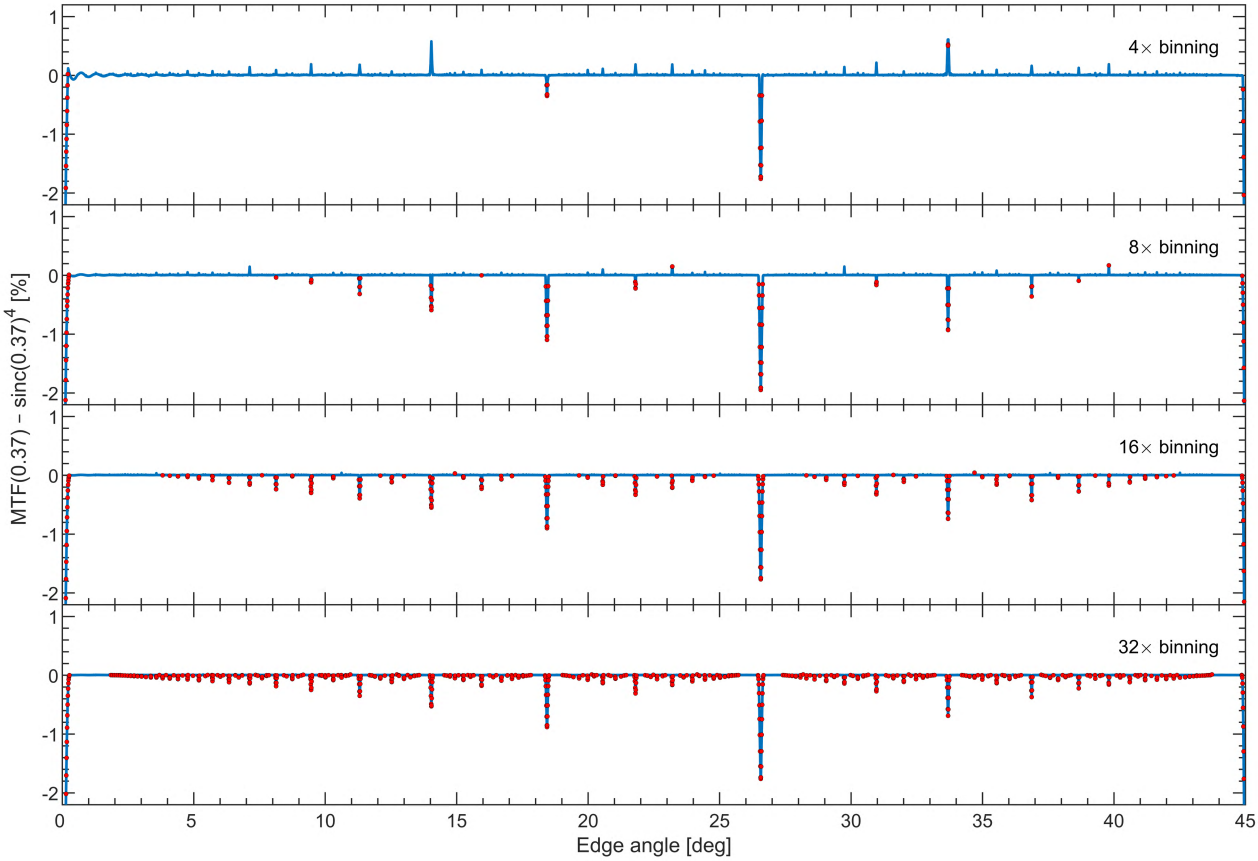

FIGURE 5. MTF errors at 0.37 cycles/pixel of the mean MTF values computed for 4×, 8×, 16×, and 32× binning at $(1024\,n_{\mathrm{bin}})^{-1}$-interval phases with the new edge-based method. Red dots indicate the edge angles that caused zero-count bins around the edge positions.

so on, for the other large oversampling ratio pairs, 8×:16× and 16×:32×. Significantly less precise MTF estimates are observed for critical edge angles because of the unevenly distributed pixels in the bins for each n_{bin}. The precision can be significantly improved by averaging the MTFs estimated with different phases. Fig. 5 shows the errors of the MTFs at 0.37 cycles/pixel averaged over the different phases at $(1024n_{\mathrm{bin}})^{-1}$ intervals for each n_{bin}. The red dots indicate that zero-count bins were found within $\pm 4n_{\mathrm{bin}}$ bins from the edge positions at any one of the 1024 different binning phases. More zero-count bins and less accurate results are observed around critical angles for higher oversampling ratios. The negative errors are due to the simple interpolation of the zero-count bins. However, the errors are significantly small, except for the critical edge angles around 0°, 45°, and $\tan^{-1}(1/2)$ (= 26.5651°). In practical edge-based MTF measurements, averaging MTFs over larger phase interval phases, such as $(32n_{\mathrm{bin}})^{-1}$ (as shown in Fig. 3) rather than $(1024n_{\mathrm{bin}})^{-1}$, would still work effectively in terms not only of precision but also of the computational cost. Without averaging MTFs at different binning phases, precision is higher with a higher oversampling ratio, as shown in Fig. 4, regardless of more zero-count bins because the shift-invariance assumption in the edge-based methods becomes more tenable with higher oversampling ratios.

E. EDGE SHIFT VARIANCE

The edge phase of the ROI image affects the accuracy of the MTF values. When the edge length is short, the shift invariance assumption in the edge-based methods becomes invalid because of insufficient edge phase variety at the sampling sites. Fig. 6 shows the mean MTF error at 0.37 cycles/pixel computed with the new edge-based method by using 4×, 8×, 16×, and 32× binning for 0.5°, 1°, and 3° slanted-edge images with an MTF characteristic of $|\mathrm{sinc}(\xi)|^4$ and ROI image heights of 1 to 100 pixels. The edge angle values were set manually. Here, the edge passed through the center of the bottom side. The MTF is significantly underestimated when the ROI image height is short because the interpolation of zero-count bins acts like lowpass filtering. It is observed that accurate MTF values are obtained when the edge phase spans more than one pixel.

F. CAMERA NOISE

In the previous sections, camera noise was not considered. Camera noise affects the accuracy of edge angle prediction,

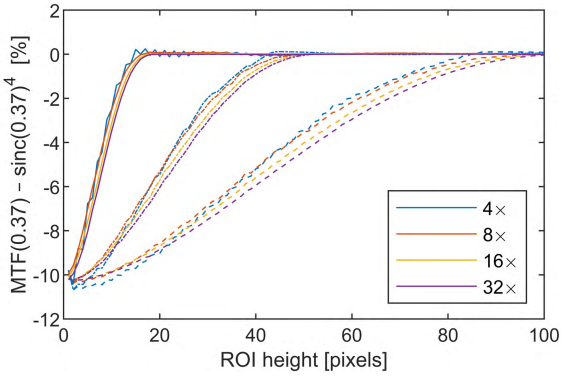

FIGURE 6. Mean MTF error at 0.37 cycles/pixel computed with the new edge-based method using 4×, 8×, 16×, and 32× binning for 0.5° (dashed lines), 1° (dash-dotted lines), and 3° (solid lines) slanted-edge images with an MTF characteristic of $|\mathrm{sinc}(\xi)|^4$ and ROI image heights ranging from 1 to 100 pixels.

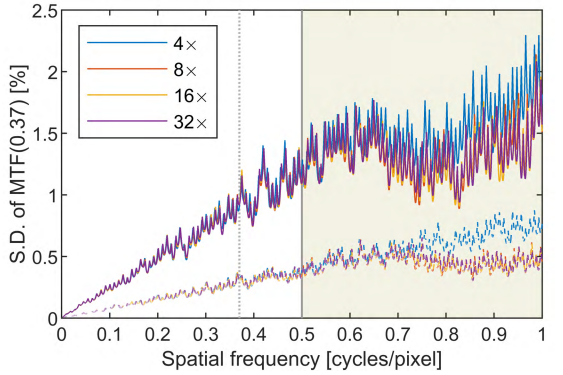

FIGURE 7. Standard deviations of MTF values at 0.37 cycles/pixel computed with 4×, 8×, 16×, and 32× binning by using the new edge-based method for 3° slanted-edge images with an MTF characteristic of $|\mathrm{sinc}(\xi)|^4$ and signal-to-noise ratios of 40 (solid lines) and 50 (dashed lines) dB.

which has a direct effect on the accuracy of the MTF estimation [12]. The algorithm for the edge angle estimation used in the new MTF measurement system is robust against camera noise [11]. Furthermore, as described in Section II.B, the system allows the user to average the first input frames for edge angle estimation such that the errors in the estimation are negligible. However, for accurate focusing, it is preferable to obtain an MTF estimate that is robust against camera noise for each frame. Fig. 7 shows the standard deviations of the MTF results at 0.37 cycles/pixel with 4×, 8×, 16×, and 32× binning by using the new edge-based method for one hundred different Gaussian noises having signal-to-noise ratios of 40 and 50 dB in a 100 (W) × 200 (H)-pixel image with a 3° slanted knife-edge passing through the image center with an MTF characteristic of $|\mathrm{sinc}(\xi)|^4$. The edge angle value was set manually. The ESFs become noisier when a higher oversampling ratio is used because the pixel counts in the bins are reduced. However, the noise affects the resultant MTF estimates at high spatial frequencies over the sampling frequency. The MTF values for a 4× oversampling ratio are rather slightly noisy around the sampling frequency because of its larger sinc-based MTF corrections than the corrections for the other oversampling ratios.

IV. CONCLUSION

This study showed that the accuracy and precision of edge-based MTF measurement methods depend strongly on the edge angle. Significantly high precision can be achieved by taking an ensemble average of MTFs computed over a single cycle of the binning phase, even at low oversampling ratios, with high accuracy through proper corrections to compensate for the attenuations of the MTF values induced by the binning and derivative processes. Even with camera noise, higher precision is achieved when a greater oversampling ratio is used in the binning process regardless of the smaller pixel counts per bin.

ACKNOWLEDGMENT

The author wishes to thank Dr. John Pincenti and Dr. Henrik Eliasson for helpful discussions on MTF corrections for the ISO 12233 edge-based method.

REFERENCES

[1] K. Masaoka, Y. Nishida, M. Sugawara, E. Nakasu, and Y. Nojiri, "Sensation of realness from high-resolution images of real objects," *IEEE Trans. Broadcast.*, vol. 59, no. 1, pp. 72–83, Mar. 2013, doi: 10.1109/TBC.2012.2232491.

[2] J. D. Gaskill, *Linear Systems, Fourier Transforms, and Optics*, 1st ed. Hoboken, NJ, USA: Wiley, 1978.

[3] F. Chazallet and J. Glasser, "Theoretical bases and measurement of the MTF Of integrated image sensors," *Proc. SPIE*, vol. 549, pp. 131–144, Jul. 1985, doi: 10.1117/12.948815.

[4] *Optics and Photonics—Optical Transfer Function—Principles of Measurement of Modulation Transfer Function (MTF) of Sampled Imaging Systems*, document ISO 15529:2010, 2010.

[5] S. K. Park, R. Schowengerdt, and M.-A. Kaczynski, "Modulation-transfer-function analysis for sampled image systems," *Appl. Opt.*, vol. 23, no. 15, pp. 2572–2582, 1984, doi: 10.1364/AO.23.002572.

[6] G. D. Boreman, *Modulation Transfer Function in Optical and Electro-Optical Systems*. Bellingham, WA, USA: SPIE, 2001, ch. 2, pp. 41–50.

[7] K. Masaoka, K. Arai, K. Nomura, T. Nakamura, and Y. Takiguchi, "Real-time measurement of ultra-high definition camera modulation transfer function," in *Proc. SMPTE Annu. Tech. Conf. Exhib.*, Los Angeles, CA, USA, 2017, pp. 1–19.

[8] *Photography—Electronic Still Picture Imaging—Resolution and Spatial Frequency Responses*, document ISO 12233:2017, 2017.

[9] S. E. Reichenbach, S. K. Park, and R. Narayanswamy, "Characterizing digital image acquisition devices," *Opt. Eng.*, vol. 30, no. 2, pp. 170–178, Feb. 1991, doi: 10.1117/12.55783.

[10] T. A. Fischer and J. Holm, "Electronic still-picture camera spatial frequency response measurement," in *Proc. IS&T ICPS*, 1994, pp. 626–629.

[11] K. Masaoka, T. Yamashita, Y. Nishida, and M. Sugawara, "Modified slanted-edge method and multidirectional modulation transfer function estimation," *Opt. Exp.*, vol. 22, no. 5, pp. 6040–6046, Mar. 2014, doi: 10.1364/OE.22.006040.

[12] P. D. Burns, "Slanted-edge MTF for digital camera and scanner analysis," in *Proc. PICS*, Portland, OR, USA, 2000, pp. 135–138.

[13] J. K. M. Roland, "A study of slanted-edge MTF stability and repeatability," *Proc. SPIE*, vol. 9396, p. 93960L, Feb. 2015, doi: 10.1117/12.2077755.

[14] H. J. Ojanen and A. Tervonen, "Method for characterizing a digital imaging system," U.S. Patent 7 499 600, Mar. 3, 2009.

[15] K. Kohm, "Modulation transfer function measurement method and results for the Orbview-3 high resolution imaging satellite," in *Proc. 20th ISPRS Congr.*, Istanbul, Turkey, 2004, pp. 7–12.

[16] *Measurement Methods for Resolution Characteristics of Television Camera Systems*, (in Japanese), document TR-B41, Association of Radio Industries and Businesses, Tokyo, Japan, Sep. 2016.

[17] J. B. Phillips and H. Eliasson, *Camera Image Quality Benchmarking*. Hoboken, NJ, USA: Wiley, 2018, pp. 200–201.
[18] J. W. Coltman, "The specification of imaging properties by response to a sine wave input," *J. Opt. Soc. Amer. A, Opt. Image Sci.*, vol. 44, no. 6, pp. 468–471, Jun. 1954, doi: 10.1364/JOSA.44.000468.
[19] M. Estribeau and P. Magnan, "Fast MTF measurement of CMOS imagers using ISO 12333 slanted-edge methodology," *Proc. SPIE*, vol. 5251, pp. 243–252, Feb. 2004, doi: 10.1117/12.513320.
[20] D. Williams, "Benchmarking of the ISO 12233 slanted-edge spatial frequency response plug-in," in *Proc. PICS Conf.*, 1998, pp. 133–136.
[21] F. van den Bergh, "Deferred slanted-edge analysis: A unified approach to spatial frequency response measurement on distorted images and color filter array subsets," *J. Opt. Soc. Am. A Opt. Image Sci. Vis.*, vol. 35, no. 3, pp. 442–451, Mar. 2018, doi: 10.1364/JOSAA.35.000442.

KENICHIRO MASAOKA received the Ph.D. degree in engineering from the Tokyo Institute of Technology in 2009. He was a Visiting Scientist with the Munsell Color Science Laboratory, Rochester Institute of Technology, in 2012, with Profs. M. D. Fairchild and R. S. Burns for a six-month residency. He is currently a Principal Research Engineer at NHK Science & Technology Research Laboratories, Tokyo, Japan. His research interests include color science and digital imaging systems. In 2017, he received the Society for Information Display Special Recognition Award for his leading contributions to the research and development of a wide-color-gamut UHD-TV display system and gamut-area metrology.